



# CHORUS

This is the accepted manuscript made available via CHORUS. The article has been published as:

## Experimental verification of a self-consistent theory of the first-, second-, and third-order (non)linear optical response

Javier Pérez-Moreno, Sheng-Ting Hung, Mark G. Kuzyk, Juefei Zhou, Shiva K. Ramini, and Koen Clays

Phys. Rev. A **84**, 033837 — Published 19 September 2011

DOI: [10.1103/PhysRevA.84.033837](https://doi.org/10.1103/PhysRevA.84.033837)

# Experimental verification of a self-consistent theory of the first-, second-, and third-order (non)linear optical response

Javier Pérez-Moreno\*

*Department of Chemistry, University of Leuven, Celestijnenlaan 200D, B-3001 Leuven, Belgium*

Sheng-Ting Hung†

*Department of Chemistry, University of Leuven, Celestijnenlaan 200D, B-3001 Leuven, Belgium, and  
Department of Physics and Astronomy, Washington State University, Pullman, Washington 99164-2814*

Mark G. Kuzyk‡

*Department of Physics and Astronomy; and Materials Science Program,  
Washington State University, Pullman, Washington 99164-2814*

Juefei Zhou§

*Department of Physics and Astronomy, Washington State University, Pullman, Washington 99164-2814*

Shiva K. Ramini¶

*Department of Physics and Astronomy, Washington State University, Pullman, Washington 99164-2814*

Koen Clays\*\*

*Department of Chemistry, University of Leuven, Celestijnenlaan 200D, B-3001 Leuven, Belgium; and  
Department of Physics and Astronomy, Washington State University, Pullman, Washington 99164-2814*

We show that a combination of linear absorption spectroscopy, hyper-Rayleigh scattering, and a theoretical analysis using sum rules to reduce the size of the parameter space leads to a prediction of the imaginary part of the second hyperpolarizability of the dye AF-455 that agrees with the experimental data gathered through two-photon absorption spectroscopy. Our procedure, which demands self-consistency between several measurement techniques and does not use adjustable parameters, provides a means for determining transition moments between the dominant excited states based strictly on experimental characterization. This is made possible by our new approach that uses sum rules and molecular symmetry to rigorously reduce the number of required physical quantities.

PACS numbers: 42.65.An, 33.15.Kr, 11.55.Hx, 32.70.Cs

## I. INTRODUCTION

There is a long history of using nonlinear-optical techniques to build an understanding of the mechanisms of light-matter interactions. Given the availability of mostly single-wavelength lasers, early measurements used time domain studies to deconvolute mechanisms such as molecular reorientation and the electronic response in liquids[1–4] which were used to make fast optical gates,[5] and in solids, for example, to study excitons in quasi-one-dimensional polymeric crystals.[6, 7]

One of the first attempts to use dispersion in the Optical Kerr Effect (OKE) to understand the nonlinear-optical response in liquids was based on a qualitative comparison of experimental results with the sum-over-states (SOS) expression for the nonlinear-optical

susceptibilities[8] as calculated by Orr and Ward.[9] More recently, OKE dispersion measurements and more sophisticated multi-state models have been applied to determining the transition moments between excited states in silicon phthalocyanine-monomethacrylate.[10]

The difficulty with such approaches is that they require either non-realistically simple models with only a couple of parameters; or, complex models that involve transition moments between excited states that can not be independently verified by experiment. Furthermore, a set of parameters that successfully models one particular measurement is not often consistent with other independent measurements.

An alternative approach that is based only on experimental characterization was proposed by Kelley, with the goal of predicting the frequency dispersion of the first hyperpolarizability of push-pull chromophores based on the linear spectrum.[11] The main drawback of such an approach is that it relies on the two-level approximation, which is not appropriate in the case of structures with more than one single transfer band peak in the linear absorption spectrum. Furthermore, the two-level model has been shown to be only valid for 1-D structures and hence does not apply to molecules with other

---

\* Javier.PerezMoreno@fys.kuleuven.be

† ShengTing.Hung@fys.kuleuven.be

‡ kuz@wsu.edu

§ jfzhou@wsu.edu

¶ rshiva@wsu.edu

\*\* Koen.Clays@fys.kuleuven.be

symmetry motifs such as octupoles.[12–14] Moreover, it has also been shown that in order to be consistent with the Thomas-Kuhn sum rules, *at least* three levels must contribute to the sum-over-states expression for the first hyperpolarizability,[15, 16] so the two-level model is inappropriate for the modeling of the nonlinear-optical response.

The sum rules are quantum mechanical identities that relate the dipole matrix elements and energies to each other; so, the SOS hyperpolarizability can be expressed in terms of a subset of the dipole matrix elements.[17–19] Indeed, the dipole-free SOS expression is derived by using the sum rules to eliminate all terms with dipole moment differences. Dipole-free expressions for both the hyperpolarizability,  $\beta$ , [20] and the second hyperpolarizability,  $\gamma$ , [21] have been derived and shown to be mathematically equivalent to the standard SOS results. These dipole-free expressions are key to significantly reducing the number of parameters required to model the nonlinear response.

In the present work, we use linear absorption spectroscopy to determine the energies and transition moments from the ground state of the octupolar chromophore commonly referred to as AF-455. Then, group theory in conjugation with the symmetry of the molecule is used to reduce the number of parameters required to describe the nonlinearity so that the dipole-free SOS expression for the hyperpolarizability can be used in conjunction with hyper-Rayleigh scattering to determine the transition moment between the two dominant states. Using *no adjustable parameters*, we predict the spectrum of the imaginary part of the second hyperpolarizability, which we show agrees with the experimental results. This suggests that our approach may be a simple alternative that is straightforward to apply and yields self-consistent results that span linear absorption, hyper-Rayleigh scattering, and two-photon absorption spectroscopy.

What makes our work unique is that all of the quantities required to predict the linear and nonlinear-optical response are determined experimentally, which is made possible using sum rules to reduce the number of required parameters. Other approaches have been proposed to provide estimates of the nonlinear response from simple measurements. For example, Pérez-Moreno and coworkers have introduced a rule of thumb that provides a rough estimate of the resonant two-photon absorption (TPA) cross-section of a large set of molecules simply using the number of  $\pi$  electrons.[22] Rebane and coworkers used a theoretical approach based on the density matrix to show that parameters determined from a measurement of the linear absorption spectrum of a dipole transition can be used to determine the TPA cross-section at the one-photon absorption maximum.[23] For a broad range of molecules, the approach was shown to yield TPA cross-sections that deviated at most by 50% compared with measurements. However, while these approximate techniques are useful for estimating the TPA cross-section, they do not predict the dispersion of the TPA cross-section, nor do they predict the first hyperpolarizability.

In contrast, the approach presented here leads to an accurate prediction of the spectrum of the imaginary part of the second hyperpolarizability, or equivalently, to an accurate prediction of the TPA spectrum.

## II. THEORY

Our approach begins by simplifying the analysis of the dispersion of the nonlinear-optical susceptibilities by providing a model that depends only on a reduced set of measurable molecular parameters. In contrast, most studies reported in the literature rely on calculating and/or using as fit parameters transition energies between excited states, excited state dipole moments, and energies.

Because excited-state parameters cannot be experimentally verified, and often many sets of parameters can yield reasonably good fits of the data to the theory, the conclusions based on such studies may not be sound. Furthermore, one set of parameters will often provide a good fit to one experiment, but not to others. To compound such problems, semi-empirical calculations of a nonlinear susceptibility that agree with off-resonance measurements often do not correctly predict the resonant behavior.

We begin by introducing the sum-over-states (SOS) dipole-free expressions of the nonlinear-optical susceptibilities. These expressions reduce the number of parameters needed to describe the nonlinear-optical response by eliminating the explicit dependence on dipole terms. Next, we explore the symmetries of the octupolar structure using group theory to reject the traditional 4-state model for planar octupoles and derive a 6-state model that is in agreement with the linear absorption spectrum. Then we use the dipole-free expressions to show how the contributions of the 6-states can be reduced to an effective 3-state model.

### A. Sum Rules and the Dipole-Free SOS Expressions

The polarizability of a molecule along  $\hat{x}$  for an incident field of frequency  $\omega$  polarized along  $\hat{x}$  is given by,[9]

$$\alpha_{xx}(\omega) = \sum_n^{\infty'} \left[ \frac{\mu_{0n}\mu_{n0}}{E_{n0} - i\hbar\Gamma_n - \hbar\omega} + \frac{\mu_{0n}\mu_{n0}}{E_{n0} + i\hbar\Gamma_n + \hbar\omega} \right], \quad (1)$$

where  $\mu_{nm}$  is the transition dipole moment along the  $\hat{x}$  direction between states  $n$  and  $m$ ,<sup>1</sup>  $E_{n0} = E_n - E_0$  is the

<sup>1</sup> A complex molecule is made of many electrons, so the dipole moment operator is proportional to a sum over the position operators of all the electrons. In matrix form, this can be expressed as  $\vec{\mu}_{ij} = -e \sum_n^N \langle \psi_i | \vec{x}^{(n)} | \psi_j \rangle \equiv -e \vec{x}_{ij}$ , where  $-e$  is the charge of the electron and  $N$  is the number of electrons in the molecule.

energy difference between states, and where the prime denotes the fact that the ground state is excluded from the sum. Notice that the energy denominators are complex to account for damping and broadening effects through the linewidths,  $\Gamma_n$ . [9] Also, the molecular susceptibilities are tensorial quantities, and for clarity we list only the expressions for the diagonal component (along the  $\hat{x}$  component).

The Thomas-Kuhn sum rules are calculated from the Schrödinger Equation using the closure identity. [24–26] For charges under the influence of electric and magnetic fields, the generalized sum rules are exactly obeyed, and are derived from the matrix elements of commutators of the Hamiltonian  $H$  and position  $x$  operators, which yields [18]

$$\frac{2m}{\hbar^2} \sum_n x_{ln} x_{np} \left( E_n - \frac{1}{2} (E_p + E_l) \right) = N \delta_{l,p}, \quad (2)$$

where  $m$  is the electron mass,  $\hbar$  is the reduced Plank constant and  $N$  is the number of polarizable electrons. Note that the set of relationships given by Equation 2 with  $l = p$  are commonly called the *sum rules*. The more general form above with  $l \neq p$  was developed to account for the off-diagonal components. [17, 18] Equation 2 corresponds to an infinite set of equations, which are each labeled by distinct pairs of integers  $l, p$ . The sum rules clearly show how the matrix elements of the position operator (which is proportional to the dipole matrix,  $\mu_{nm} = -ex_{nm}$ ) and energy levels are intimately related to each other and therefore can not be independently adjusted.

The infinite set of equations embedded in the sum rules can be used to simplify the SOS expressions for the nonlinear-optical susceptibilities. The off-diagonal sum rules of the type  $(l, p) = (0, i)$  with  $i = 1, 2, 3, \dots$  can be used to express the ground and excited state dipole moments in terms of transition moments. [20] As such, the explicit dependence on dipole terms can be eliminated. [20] Using these relationships, the traditional SOS expressions can be transformed into dipole-free SOS expressions, which for the largest diagonal component of the first hyperpolarizability yields, [20]

$$\beta_{xxx}(\omega_1, \omega_2) = \sum_m' \sum_{n \neq m}' \frac{\mu_{0m} \mu_{mn} \mu_{n0}}{D_{nm}^{-1}(\omega_1, \omega_2)} \quad (3)$$

$$\times \left[ 1 - \frac{D_{nm}^{-1}(\omega_1, \omega_2)}{D_{nn}^{-1}(\omega_1, \omega_2)} \left( 2 \frac{E_{m0}}{E_{n0}} - 1 \right) \right],$$

where,

$$D_{nm}(\omega_1, \omega_2) = \frac{1}{2} \left[ \frac{1}{(E_{n0} - i\hbar\Gamma_n - \hbar\omega_1 - \hbar\omega_2)(E_{m0} - i\hbar\Gamma_m - \hbar\omega_1)} \right. \\ \left. + \frac{1}{(E_{n0} + i\hbar\Gamma_n + \hbar\omega_2)(E_{m0} - i\hbar\Gamma_m - \hbar\omega_1)} \right]$$

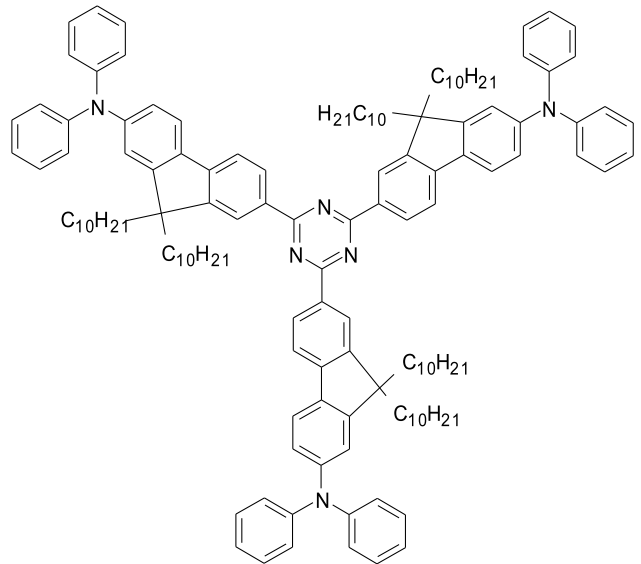


FIG. 1. The chemical structure of the AF-455 molecule. Notice that the relevant symmetry for the optical response is  $D_{3h}$ .

$$+ \frac{1}{(E_{n0} + i\hbar\Gamma_n + \hbar\omega_2)(E_{m0} + i\hbar\Gamma_m + \hbar\omega_1 + \hbar\omega_2)} \\ + \text{Permutations of } \omega_1 \leftrightarrow \omega_2 \text{ for the previous terms}]. \quad (4)$$

This expression is sometimes called the reduced SOS expression.

The second hyperpolarizability, as well as higher-order hyperpolarizabilities, can be transformed into a dipole-free form. The resulting algebraic expressions are too complex to present here, but their form can be found in the literature. [21]

## B. The molecular symmetry of AF-455

We will now consider the symmetry properties of the AF-455 chromophore in order to define the energy level diagram and to find an appropriate symmetry-adapted basis that is consistent with the linear absorption data. The chemical structure of the AF-455 chromophore is shown in Fig. 1. First we notice that although strictly speaking, the symmetry of the overall structure is  $C_{3h}$ , for all the optical properties the effective or relevant symmetry is dictated by the symmetry of the planar conjugated part of the molecule. That is, for optical purposes, the relevant symmetry of the molecule is  $D_{3h}$ .

Our next step is to define an appropriate basis that would allow us to determine the energy level diagram with the aid of group theory. Since we demand self-consistency with all the experimental data, we need first to consider the structure of the linear absorption data of the molecule in solution (tetrahydrofuran), shown in Fig. 2. The linear spectrum clearly shows two broad bands.

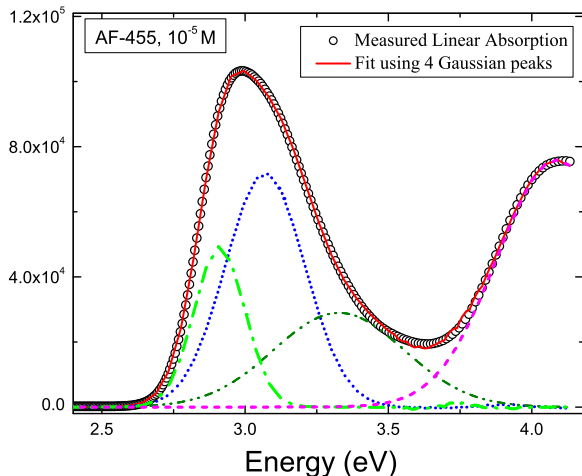


FIG. 2. (Color online) Linear absorption spectrum of AF-455 in solution in tetrahydrofuran (black open circles), and fit using four Gaussians (red line). The individual Gaussian functions are also shown; three to fit the first excited state - (dark green dash-dot), (blue dots) and (light green dash-double dot) - and one for the second excited state (pink dash).

For a complex molecule such as AF-455, each band might be the result of many closely-lying excited states, with coupling between vibronic and electronic states. While in principle, low-temperature linear spectral characterization could be used to resolve the electronic structure, such an approach would go against our principle of demanding self-consistency between the different measurement techniques given that the second- and third-order experiments are performed at room temperature. Therefore, our self-consistent approach demands that we model the response in terms of the two broad bands that are present in the linear absorption spectrum at room temperature. As we shall see, the use of the dipole-free expressions together with the Franck-Condon approximation allows us to model the dispersion using effective levels that each might be a composite of closely-lying states.

Our initial choice of basis set should result in an energy level diagram that is compatible with the experimental linear absorption spectrum. It is customary to model planar octupolar structures with  $D_{3h}$  symmetry using a set of 4 basis states, as sketched in Fig. 3.[12, 27, 28] Although such an approach leads to an energy diagram with three energy levels (see Fig. 3), the symmetry of the states does not allow  $(x, y)$  transitions between the ground and the first excited level,[12] and therefore, the linear absorption spectra would only show one peak (for details on the group theory calculations, please refer to section B 1 in the appendix). Hence, based on the empirical evidence we rule out this traditional choice of basis. Furthermore, the central ring (s-triazine) can not be represented by the same type of basis used for the branches. While each of the branches has only 1  $p_z$  orbital at the

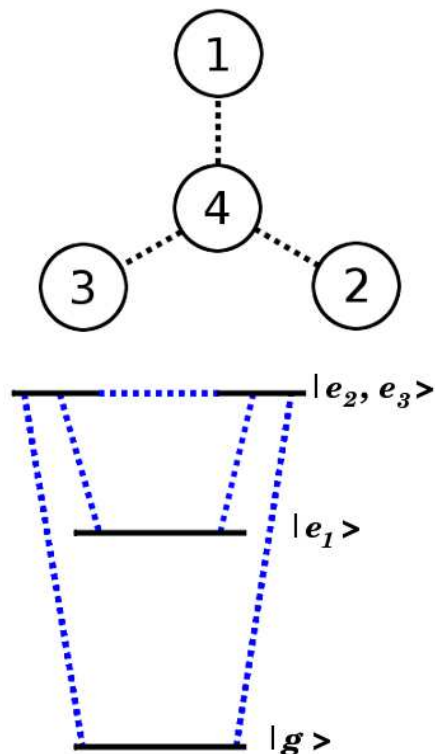


FIG. 3. (Color online) The 4-basis set that is traditionally used for the modeling of charge-transfer octupolar structures with  $D_{3h}$  symmetry (top) and the resulting energy level diagram (bottom). Using group theory, the 4-basis set shown on the top are transformed by a linear combination into 4 symmetry adapted basis states (SALC). Allowed  $(x, y)$  transitions are shown as dotted lines. This choice of basis has only one  $x$  allowed transition connecting the ground state  $|g\rangle$  and an excited state  $|e_2, e_3\rangle$  (which is doubly degenerate) and therefore is inconsistent with the observed two-band linear absorption spectrum.

end of the conjugated path, the central ring has 3  $p_z$  orbitals and therefore they do not form an equivalent basis set.<sup>2</sup>

Our choice of basis set must still be consistent with  $D_{3h}$  symmetry of the AF-455 chromophore but must include an additional independent state in order to generate enough  $(x, y)$  allowed transitions to be in agreement with the linear absorption spectrum. Focusing on the position of the  $p_z$  orbitals associated with every Nitrogen in the structure, we introduce a set of 6 basis states as shown in Fig. 4 (top). From this choice of basis set, and using group theory, the symmetry-adapted basis that is

<sup>2</sup> If we had started only with three initial basis states (each one corresponding to the  $p_z$  orbital at the end of the branch) as is typical in the literature,[29] there would be only one excited state energy (doubly degenerate), which is inconsistent with the linear absorption data.

generated has an energy level diagram compatible with the linear absorption spectrum provided that two of the excited states are close in energy such that they cannot be resolved in the linear absorption spectrum. By inspecting the resulting symmetry-adapted basis set (section B 2 in the appendix) we can indeed justify this condition. The original set of bases can be separated into two subgroups, a set that spans the wavefunctions related to excitations along the long conjugated branches (labeled as  $|1\rangle$ ,  $|2\rangle$  and  $|3\rangle$  in Fig. 4) and another set that spans the wavefunctions related to excitations along the conjugated central ring (labeled as  $|4\rangle$ ,  $|5\rangle$  and  $|6\rangle$ ). In the absence of perturbations the central ring would be aromatic and therefore extremely stable. Consequently, it will take much more energy to generate an excited state that breaks the aromaticity than to generate a charge transfer through the long branches.

We can estimate the energy ratio between the energies involved in the transitions within the branches (of order  $\delta$ ) to the energies involved in the transitions within the ring (of order  $\Delta$ ) by comparing the different sizes of the unperturbed systems. A generic result of quantum mechanics that relates the length of confinement of the wavefunction ( $L$ ) with its energy,  $E \propto L^{-2}$ , can be used to calculate the ratio between the two energies as:

$$\frac{\delta}{\Delta} \propto \frac{(\text{ring radius})^2}{(\text{branch length})^2} \approx \frac{1}{10^2} = \frac{1}{100}. \quad (5)$$

We thus conclude that our choice of basis set is consistent with the results from the linear characterization experiments: the linear absorption spectrum shows the transitions between 3 effective bands, which correspond to 6 electronic levels, ground, first effective excited state (made up from 3 closely-lying states) and second excited state (made up of two degenerate states) as shown schematically in Fig. 4.

### C. Using effective levels with the dipole-free expressions: effects of closely-lying states upon the hyperpolarizabilities

In the previous section (section II B) we have argued that the symmetry of the AF-455 chromophore results in a 6-state model that behaves as an effective three-level model in the linear absorption. Now we will show how we can model the hyperpolarizabilities in terms of these effective states. Specifically, we will use the dipole-free SOS expression for the first hyperpolarizability (Eq. 3) to show that when a peak in the linear absorption spectrum is made up of the contributions from close-lying states, these close-lying states act as one “effective” excited state for the purpose of modeling the linear and nonlinear optical response. In particular, in the limit when the closely-lying states are degenerate, the optical observables can be modeled by treating each set of degenerate states as one “effective” excited state.

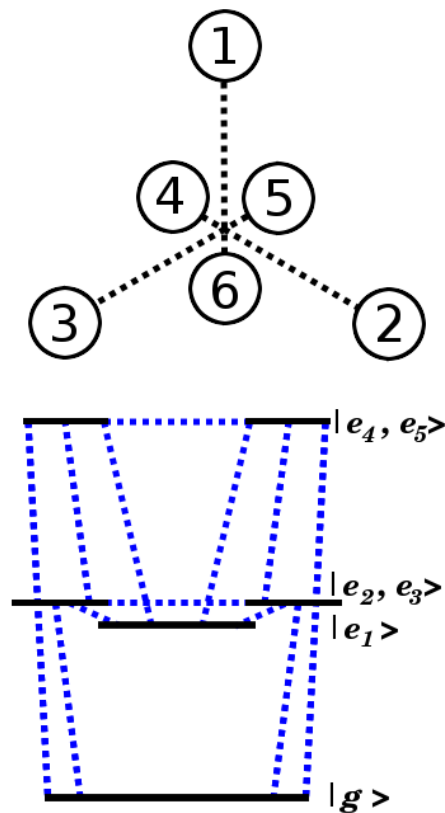


FIG. 4. (Color online) The 6-member basis set that we propose for the modeling of charge-transfer octupolar structures with  $D_{3h}$  symmetry and a central ring (top) and the resulting energy level diagram (bottom). Using group theory, the 6 original basis shown on the top are transformed by a linear combination into a 6-state symmetry-adapted basis (SALC). Allowed  $(x,y)$  transitions are shown through dotted lines. Notice that the energy difference between the first ( $|e1\rangle$ ) and second excited state ( $|e2, e3\rangle$  which is doubly degenerate) is much smaller than the energy difference between the rest of the states, and therefore this choice of basis will show two effective bands in the linear absorption spectrum, in agreement with the experimental linear characterization.

We start by assuming that each peak in the linear absorption spectrum is made of contributions from a set of closely-lying states. By superposition, the contribution of close-lying states can add to appear like the contribution of one “effective” single state. Mathematically, if  $|1'\rangle$ ,  $|2'\rangle$ ,  $\dots$   $|k'\rangle$  denote the closely-lying states that result in the “effective” state  $|I\rangle$ , then it follows that:

$$\sum_{i'=1}^{k'} \mu_{gi'} \mu_{i'g} \cdot d_{i'}^{(1)}(\omega) \approx \mu_{gI} \mu_{Ig} \cdot d_I^{(1)}(\omega), \quad (6)$$

where the linear dispersion terms  $d_n^{(1)}$  are defined by:

$$d_n^{(1)}(\omega) = \left\{ \frac{1}{E_{n0} - i\hbar\Gamma_n - \hbar\omega} + \frac{1}{E_{n0} + i\hbar\Gamma_n + \hbar\omega} \right\}, \quad (7)$$

in agreement with Eq. 1.

Next we consider the contributions from the closely-lying states to the first hyperpolarizability. The dipole-free expression for the first hyperpolarizability (Eq. 3) can be expressed as:

$$\beta_{xxx}(\omega_1, \omega_2) = \sum_n' \sum_{m \neq n}' \mu_{0n} \mu_{nm} \mu_{m0} \cdot D_{mn}(\omega_1, \omega_2), \quad (8)$$

Two types of terms contributing to Eq. 8 are:

- Terms that do not couple closely-lying states, which are of the type  $\mu_{0i} \mu_{ij'} \mu_{j'0} \cdot D_{ij'}(\omega_1, \omega_2)$  or  $\mu_{0i'} \mu_{i'j} \mu_{j0} \cdot D_{i'j}(\omega_1, \omega_2)$ .
- Terms that couple the closely-lying states, which are of the type  $\mu_{0i'} \mu_{i'j'} \mu_{j'0} \cdot D_{i'j'}(\omega_1, \omega_2)$ .

Note that the primed indices refer to the set of nearly-degenerate states.

The first type of contribution (with no coupling between closely-lying states) can be rewritten in terms of one effective state. For example, consider all the processes for which there is a transition from the ground state  $|0\rangle$  to state  $|1\rangle$ , then from  $|1\rangle$  to one of the closely-lying states  $\{|i'\rangle\}_{i'=1', \dots, k'}$  and then back to the ground state:

$$\sum_{i'=1'}^{k'} \mu_{01} \mu_{1i'} \mu_{i'0} \cdot D_{i'1}(\omega_1, \omega_2) = \quad (9)$$

$$\mu_{01} \left( \sum_{i'=1'}^{k'} \mu_{1i'} \mu_{i'0} \cdot D_{i'1} \right) \approx \mu_{01} \mu_{1I} \mu_{I0} \cdot D_{I1}.$$

When all these terms are summed, they can be approximated as a transition to the “effective” state  $|I\rangle$  in the same manner as in the linear case (Eq. 6).

A problem arises from terms that couple closely-lying states because they cannot be re-expressed with an “effective” single state. For example, consider:

$$\mu_{0i'} \mu_{i'j'} \mu_{j'0} \cdot D_{i'j'}(\omega_1, \omega_2). \quad (10)$$

Recalling the definition of the dispersion factor  $D_{i'j'}$  (Eq.4):

$$D_{i'j'}(\omega_1, \omega_2) = \quad (11)$$

$$\left( \frac{1}{D_{j'i'}^{-1}(\omega_1, \omega_2)} - \frac{1}{D_{i'j'}^{-1}(\omega_1, \omega_2)} \left\{ 2 \frac{E_{i'0}}{E_{j'0}} - 1 \right\} \right).$$

Since states  $|i'\rangle$  and  $|j'\rangle$  are of nearly the same energy,  $D_{i'j'} \approx D_{j'i'}$  and  $E_{i'0} \approx E_{j'0}$ , and Eq. 11 reduces to:

$$D_{i'j'}(\omega_1, \omega_2) \approx \quad (12)$$

$$\left( \frac{1}{D_{i'i'}^{-1}(\omega_1, \omega_2)} - \frac{1}{D_{i'i'}^{-1}(\omega_1, \omega_2)} \{2 - 1\} \right) = 0.$$

Thus, the contributions of such terms to the hyperpolarizability are negligible so the SOS expression for

the hyperpolarizability reduces to an effective three-level model. In the case of truly-degenerate states, there is no coupling between them, so they do not contribute to the hyperpolarizability. A similar argument applies to the expression for the second hyperpolarizability.

So far we have considered only the effects of closely-lying and degenerate electronic levels upon the hyperpolarizabilities. While it is clear that the same principle would apply for closely-lying vibronic states, it could be argued that our reasoning does not hold for vibronic states within the same electronic band if their spacing is large enough. In principle such contributions should be negligible because the transition dipole moments corresponding to transitions between vibronic states are usually orders of magnitude smaller than electronic transition moments. However, we will assume that to first order the Franck-Condon approximation applies to AF-455, implying that transitions between vibronic states on the same electronic band are disallowed or that they lead to negligible contributions to the hyperpolarizabilities. Since these are the only types of transitions that we might miss by modeling the hyperpolarizabilities in terms of “effective” states, we can use our self-consistent procedure as a test of the validity of the Franck-Condon approximation for the description of the optical properties of the AF-455 chromophore.

### III. RESULTS AND DISCUSSION

We have shown how the symmetries of the AF-455 chromophore in combination with group theory lead to a 6-state model that is in agreement with the linear absorption spectrum and behaves as an effective 3-state model. Using the dipole-free expressions, we have shown that the contributions of the 6 states can also be modeled in terms of the effective 3-state model. This leads to a model of the linear and nonlinear susceptibilities that depends only on the energy differences between the two excited states and the ground state,  $E_{10}$ ,  $E_{20}$ ; their widths; and the corresponding transition moments  $\mu_{01}$ ,  $\mu_{02}$ , and  $\mu_{12}$ . The quantities  $E_{10}$ ,  $E_{20}$ ,  $\mu_{01}$ , and  $\mu_{02}$  can be determined using the linear absorption spectrum. The only remaining unknown quantity is  $\mu_{12}$ . The transition moment between the two excited states can be determined from a measurement of the first hyperpolarizability at one wavelength provided that the other quantities are known *a priori*. From these measured quantities, we will show that all optical and nonlinear-optical properties are predicted with no adjustable parameters.

We now apply this technique to the octupolar molecule AF-455 in solution. The choice of AF-455 as a test of our methodology is motivated by its group symmetry ( $C_{3h}$ ), where one can directly determine the values of the tensorial components of the molecular polarizabilities from measurements in solution. In addition, the linear spectrum is characterized by two clearly distinguishable broad bands in the visible range making it possible to de-

termine the energies and transition moments for a three-level model analysis; and, the molecule has a measurable second- and third-order NLO response in a frequency range that is easily accessible by experiment. Also, AF-455 is a fluorescent molecule, which allows its TPA cross-section spectrum to be characterized using two-photon excitation fluorescence.

The absorption spectrum is used to determine its polarizability using the fact that with appropriate choice of molecular coordinate system,  $\alpha_{xx} = \alpha_{yy}$  and  $\alpha_{xy} = \alpha_{yx} = 0$ . Our analysis holds generally for any octupolar molecule with  $D_{3h}$  symmetry, which we will refer to simply as an octupole. An isotropic solution of octupoles will have an isotropic polarizability of  $\langle \alpha \rangle = 2\alpha_{xx}/3$ . Thus, from an absorption spectrum, the polarizability along  $\hat{x}$  can be directly determined.

The linear absorption spectrum of a sample is obtained by measuring the transmittance of a broad spectrum source passing through a cuvette of 1cm path length, and containing a solution of the sample in solvent. The spectrum is referenced to the transmittance through pure solvent in an identical cuvette. The measured linear absorption spectrum of AF-455 in tetrahydrofuran (THF) is shown in Fig. 2.

The two peak positions are used to determine the energies  $E_{10}$  and  $E_{20}$ ; and the width at half maximum for each peak is used to determine  $\Gamma_1$  and  $\Gamma_2$ . The absorption spectrum is fit to four Gaussian peaks; three for the first excited state and one for the second excited state as shown in Figure 2. The sum of the areas of the first three peaks is used to calculate the transition moment to the first excited state, using the method described by Tripathi et al,[30] while the area of the fourth Gaussian is used to get the transition moment to the second excited state. The solid curve is the sum of all four peaks, and shows that the four-Gaussian theory provides a good fit to the data. The results are summarized in Table I.

The first hyperpolarizability is determined through hyper-Rayleigh scattering (HRS), using a femtosecond pulsed laser (Millennia X + Tsunami with a lock-to-clock system that ensures 80MHz pulsed output) at a fundamental wavelength of  $\lambda = 800nm$  in conjugation with a low-frequency lock-in amplifier and a signal generator. Details can be found elsewhere.[31, 32] The measured HRS hyperpolarizability, using the  $90^\circ$  geometry, yields,

$$\langle \beta_{HRS}^2 \rangle = \frac{8}{21} \beta_{xxx}^2. \quad (13)$$

The octupolar symmetry of the compound (which is used in Equation 13 to determine  $\beta_{xxx}$  directly from an HRS measurement) was confirmed by the depolarization measurements. Note that the other components of the  $\beta$  tensor are given by,[33]

$$\beta_{xxx} = -\beta_{xxy} = -\beta_{xyx} = -\beta_{yxx}, \quad (14)$$

while all other tensor components vanish. A demodulation technique is used to determine a fluorescence-free

value to insure that only the hyperpolarizability is being measured.[34] We note that for AF-455, no fluorescence contribution was found at 400nm, which leads to a more accurate determination of the first hyperpolarizability than is possible with the demodulation technique when fluorescence is present.

The dipole-free expression for the diagonal component of the first hyperpolarizability (Eq. 3) for a three-state model is given by:

$$\beta_{xxx}(\omega_1, \omega_2) = \sum_{n=1}^2 \sum_{m \neq n}^2 \mu_{0n} \mu_{nm} \mu_{m0} \cdot D_{mn}(\omega_1, \omega_2), \quad (15)$$

with the dispersion functions,  $D_{nm}(\omega_1, \omega_2)$  as defined in Eq. 4 and  $\mu \equiv -ex$ . In the HRS measurement,  $\omega_1 = \omega_2 = \omega$ . We note that for an infinite number of states, the standard SOS and dipole-free expressions are rigorously identical; but when truncated to three states, the two are different. It is not possible *a priori* to know which expression is more accurate. Our strategy is to use the dipole-free expression because it does not require knowledge of the dipole moments. The merits of this approach will be judged by the predictive capability of the model.

The linear absorption measurement determines all the transition moments, energies and widths except for  $\mu_{12}$ . Thus, given that the first hyperpolarizability is measured at a known frequency  $\omega$ , Eq. 15 can be inverted to solve for  $\mu_{12} = -ex_{12}$ . Table I shows all of the parameters determined from linear absorption spectroscopy and the measurement of the first hyperpolarizability at a fundamental wavelength of  $800nm$ . The three values of  $\mu_{12}$  listed in Table I represent the uncertainty range due to uncertainty in the HRS measurement.

Figure 5 shows the experiment used for determining the TPA cross-section from the measured two-photon fluorescence power, a technique that was developed by Xu and Webb.[35] Details of how the data is related to the two photon cross-section can be found in the original paper.[35] The advantage of this experiment is that it is a reliable method for determining the TPA cross-section[36] and is not as susceptible to excited state absorption as is nonlinear transmission.[37, 38] Here we briefly describe the issues that are particular to our implementation of the technique.

The sample solution is prepared by adding 0.0958 gram of AF-455 crystals as received from Wright Patterson Air Force Base to 200ml optical spectrum grade THF, in a clean flask at room temperature. The mixture is agitated in an ultrasonic water bath for thirty minutes to make a uniform solution. Two quartz cuvettes (ordered as a matched pair) are filled, and labeled S1 and S2, respectively, are filled to 4/5 full with the uniform solution. These two identical samples are used to calibrate the collection efficiency of the reference and sample arms of the TPA experiment.

The reference solution is made from 200ml of 100M Rhodamine B solution by adding 0.00958 grams of Rho-

$E_{10}$ (eV)	$E_{20}$ (eV)	$ \mu_{10} $ (D)	$ \mu_{20} $ (D)	$\Gamma_{10}$ (eV)	$\Gamma_{20}$ (eV)	$ \mu_{12} ^{\text{upper}}$ (D)	$ \mu_{12} ^{\text{middle}}$ (D)	$ \mu_{12} ^{\text{lower}}$ (D)
3.0	4.1	12.6	9.4	0.22	0.35	15.5	12.6	9.7

TABLE I. Experimental parameters (from the linear absorption spectrum) and  $|\mu_{12}|$  measured using HRS. The range of  $|\mu_{12}|$  values (upper, middle and lower) reflect the experimental uncertainties associated with HRS. All quantities are local-field corrected values.

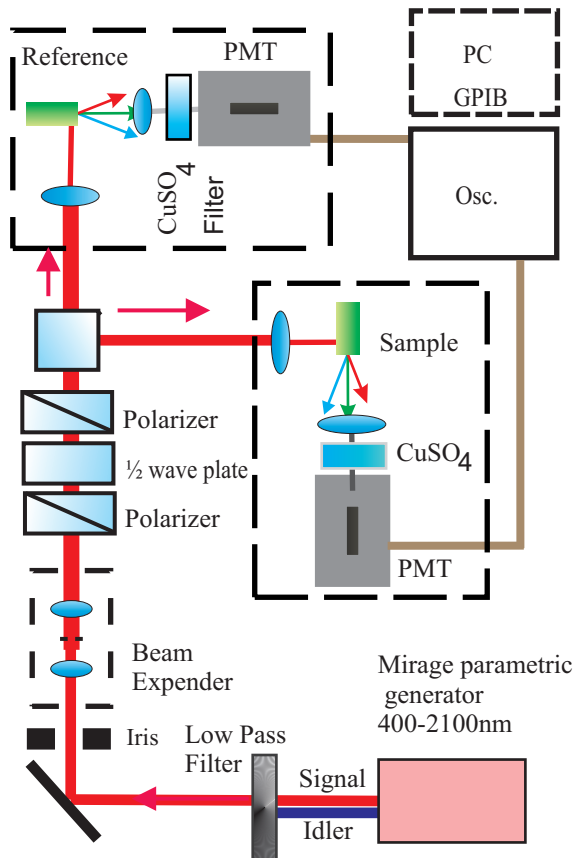


FIG. 5. (Color online) Schematic representation of the experiment used for measuring the two-photon absorption cross-section.

damine B powder to 200ml optical spectrum grade methanol followed by agitation in an ultrasound bath for 30 minutes at room temperature. A clean cuvette is filled with this solution to 4/5 full and capped tightly.

A sample is excited with a laser beam, and the two-photon fluorescence signal (integrated over all fluorescence wavelengths) is detected with an RCA C31034A-02 photomultiplier tube (PMT). This PMT is of high quantum efficiency over a broad range of wavelengths throughout the visible. Filters are used to remove any wavelengths corresponding to the pump energy or less, leaving only the fluorescence spectrum due to two-photon absorption. The time-integrated current from the PMT is proportional to the number of two-photon absorptions. A typical run uses the average over many lasers pulses of

the 10 Hz laser source to decrease noise. The reference is used to take into account laser fluctuations and is used as a standard for determining the absolute two-photon absorption cross-section.

We are able to compute the TPA cross-section of our unknown compound (AF-455) by comparing the collected fluorescence signal from both the unknown compound and a reference, provided that the TPA cross-section of the reference is known. We use a standard reference, Rhodamine B, whose TPA cross-section dispersion in the visible region had been previously characterized by Xu and Webb.[35]

In addition to the TPA cross-section of the reference, this technique also requires knowledge of the fluorescent quantum yield of both the reference and the unknown compound; or more precisely, the ratio of their effective quantum efficiencies. This ratio could not be obtained from the literature for the range of concentrations used in our experiments. Therefore, we characterized the effective quantum efficiency ratio using one-photon excited fluorescence spectroscopy, and extrapolated the results to the two-photon regime, assuming that the one- and two-photon quantum yields are the same since the emission originates in the same excited state. We stress that such an assumption is valid only for complex organic molecules with broad bands where the quantum selection rules are relaxed; but, not for a simple atom where strict selection rules apply.

The TPA cross-section of a microscopic unit,  $\sigma_2$ , is directly related to the imaginary part of the second hyperpolarizability tensor,  $\gamma_{xxxx}(-\omega; \omega, \omega, -\omega)$ :

$$\sigma_2 = \frac{16\pi^2\hbar}{n^2\lambda^2} \langle \text{Im}[\gamma_{xxxx}^*(-\omega; \omega, \omega, -\omega)] \rangle, \quad (16)$$

where  $n$  is the refractive index of the solvent,  $\omega$  and  $\lambda$  are, respectively, the frequency and the wavelength of the fundamental beam; and  $c$  is the speed of light. Local field effects result in an effective “dressed” second hyperpolarizability ( $\gamma_{xxxx}^*$ ), which is directly related to the vacuum second hyperpolarizability through a local field factor.[39] Notice that in Eq. 16, the brackets indicate the orientational average over all the possible tensor components. However, for molecules with  $D_{3h}$  symmetry, the tensor components are related to each other:[33]

$$\gamma_{xxxx} = \gamma_{yyyy} = 3\gamma_{xyxy} = 3\gamma_{xyyx} = \text{etc} \dots, \quad (17)$$

such as it is possible to derive a direct relationship between the measured orientational average, and the

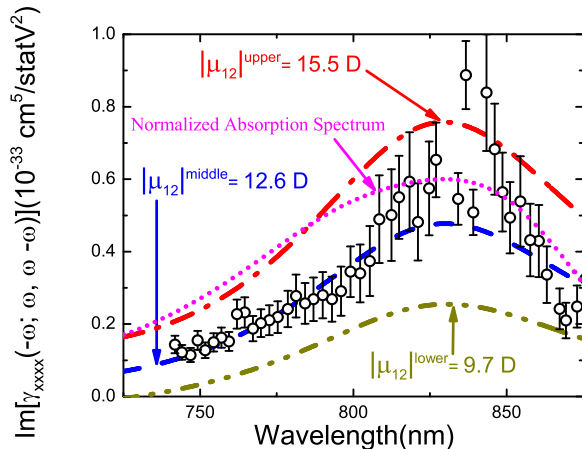


FIG. 6. (Color online) The measured spectrum of the imaginary part of the second hyperpolarizability (points) and the theoretical curve (middle), that is predicted from the measured value of  $\mu_{12}$  ( $|\mu_{12}|^{\text{middle}}$ ). The upper and lower curves represent the uncertainty in the HRS-determined transition moment  $\mu_{12}$ . Note that there are *no adjustable parameters* in the theoretical modeling. The linear absorption spectrum, shifted by a factor of 2 with respect to the wavelength and normalized to the peak is shown for comparison.

diagonal component of the second hyperpolarizability. In this manner, we can directly measure the spectrum of the imaginary part of the second hyperpolarizability,  $\text{Im}[\gamma_{xxxx}(-\omega; \omega, \omega, -\omega)]$ , and compare it with the spectrum predicted by the theory. The spectrum of  $\text{Im}[\gamma_{xxxx}(-\omega; \omega, \omega, -\omega)]$  is predicted by substituting the experimentally characterized values for the energies, transition moments and linewidths (Table I) into the SOS expression for the second hyperpolarizability. We use the *dipole-free expression* to calculate  $\gamma_{xxxx}$  because it does not require knowledge of the ground and excited state dipole moments.[21] We do not present the dipole-free-expression here, but rather refer the reader to the literature.[21]

Figure 6 shows the theoretically-calculated value of the imaginary part of  $\gamma_{xxxx}$ , as a function of wavelength using the measured values of the dipole moment matrix elements, energies, and widths shown in Table I. The upper and lower curves show the uncertainty range due to the experimental uncertainty in determining the excited state transition moment  $\mu_{12}$  using the HRS experiment.

The TPA spectrum was measured with the two-photon fluorescence experiment, which yielded an isotropic average over all tensor components of the two-photon absorption spectrum. Given the  $D_{3h}$  symmetry of the molecule, the isotropic value can be related to the individual tensor components. Thus, the measured TPA cross-section can be related directly to the imaginary part of  $\gamma_{xxxx}$ .

All of the optical characterization experiments are performed in solution, so for each order (linear, second- and

third-order), the measured quantity is an isotropic orientational average over all the possible tensor components that contribute to the response. For a molecule with  $D_{3h}$  symmetry, the relationships between the non-zero tensor components allow us to compute directly the value of the diagonal components of the polarizabilities ( $\alpha_{xx}$ ,  $\beta_{xxx}$  and  $\gamma_{xxxx}$ ) from the measured orientational average.[33] As previously mentioned, the measurement of the depolarization ratio through HRS using the  $90^\circ$  geometry,[31, 32] confirmed that AF-455 belongs to the  $D_{3h}$  symmetry group, and hence that we can trust the values of  $\alpha_{xx}$ ,  $\beta_{xxx}$  and  $\gamma_{xxxx}$  that were obtained through orientational averaging.

The measured values of the diagonal tensor components determined from isotropic averaging as described above are shown as points with error bars in Figure 6. We note that since the samples used in all measurements are liquid solutions, all quantities such as the polarizability, hyperpolarizability, transition dipole moments, etc. are dressed values.[39] Vacuum quantities are then determined using the appropriate local field models.[39]

The theoretical spectrum and the data are in good agreement and all but one of the data points fall within the error band of the predicted spectrum. Thus, the approach of using the dipole-free expressions for the first and second hyperpolarizability provides a theoretical description that is consistent with three sets of measurements. In particular, the *magnitude* of the predicted spectrum of the imaginary part of the second hyperpolarizability through the two-photon resonance is consistent with the data. While a two-photon resonant peak is expected in the vicinity of 826 nm (when  $2\hbar\omega = 3eV$ ), the shape and the strength of the peak around the resonances are very sensitive to the values of the transition moments and the linewidths. For example, if the measured value of  $\mu_{12}$  ( $|\mu_{12}|^{\text{middle}}$ ) is increased or decreased by more than 25%, the theoretical prediction would completely miss the experimental data. This suggests that our approach may be useful in modeling the dispersion of the linear and nonlinear susceptibilities of octupolar molecules with  $D_{3h}$  symmetry.

In light of the fact that AF-455 is a complex molecule, it may appear somewhat surprising that the magnitude of the predicted spectrum of the imaginary part of the second hyperpolarizability using an effective three-level model is in such good agreement with the data. This may be due to several factors. First, the HRS measurement was determined near the two-photon resonance, where the TPA peak is measured so the contributions of the first excited states are heavily weighted and dominate the response. In contrast, an off-resonant HRS measurement potentially includes contributions from the tails of many higher-energy excited states, thus yielding an inaccurate determination of the transition moment  $\mu_{12}$ . On-resonance measurement insures that the influence of the transition moment  $\mu_{12}$  is large. Since the TPA spectrum is measured only near the two-photon resonance, the same set of states are being probed. This set of states

is well modeled by treating the close-lying states as one “effective” state, which as we argued in section II C implies that the Franck-Condon approximation is valid for the description of the optical response of our molecule. Finally, it is possible that the observed agreement is a coincidence. Similar studies of other octupolar systems would determine the general applicability of our method.

It is instructive to apply the same approach to the three-level model using the standard SOS expressions under the assumption that the three states are non-degenerate and have no dipole moment. Using the value of  $\mu_{12}$ , determined from HRS measurements and the standard SOS expression for the hyperpolarizability, the theoretical value of the second hyperpolarizability predicts a two-photon absorption spectrum that is two-orders of magnitude larger than the measured one. This illustrates how the typical approach can lead to inaccurate results, and supports our argument that the dipole-free expression may be appropriate for such systems.

We also note that our theory correctly predicts the shape of the TPA spectrum. It is common practice to shift the absorption spectrum by a factor of two to approximate the TPA spectrum. The dotted curve in Figure 6 was calculated in this way, and the peak renormalized to fit the data. Clearly, the shape is not the same as the TPA data. This is not surprising because the TPA spectrum depends also on transitions between excited states and products of energy denominators while the linear absorption spectrum depends only on transitions from the ground state to individual excited states. Thus, since our theory predicts both the magnitude and shape of the spectrum, the approach is a promising one for self-consistently modeling the first three orders of (non)linear susceptibilities.

Finally, we should point out that our results can be used to propose a new strategy for the optimization of octupolar structures. The presence of the central conjugated ring with the three nitrogens demands that the basis set be chosen to span the states of the molecule to include the subset of the three basis states that span the ring. Due to the fact that the conjugated branches are much longer than the radius of the conjugated central ring, the three excited states (one of them doubly degenerate) that result from the basis subset that spans the branches are close in energy in comparison to the energy of the other excited states. In the limit when the ratio between the length of the branches and the ring radius becomes large, the three excited states would become closer in energy, so the system would better approximate a true three-level system, with allowed  $(x, y)$  transitions between the levels.

According to the three-level ansatz,[40] the intrinsic nonlinear optical response is optimized when only two-excited states contribute to the optical response. By increasing the ratio between the length of the branches and the size of the central ring, true octupolar systems could get closer to the ideal three-level system, which would maximize the intrinsic nonlinear response.

## IV. CONCLUSION

We have introduced an approach that combines measurements, symmetries, and sum rules to fully characterize the important states of a molecule that allows all of the linear and nonlinear susceptibilities to be accurately modeled with no adjustable parameters. Our approach is general in that it can be applied to any molecule of any symmetry class. In the present work, we have illustrated this approach for an octupolar molecule of  $D_{3h}$  symmetry that is modeled using three effective excited states. We have used the dipole-free forms of the SOS expressions for the first and second hyperpolarizabilities, which are derived from the sum rules and do not require knowledge of the ground and excited state dipole moments.

We have shown that the presence of a central conjugated ring in a system with  $D_{3h}$  symmetry results in an effective three-level model whose dipole matrix and energies can be fully characterized using linear absorption spectroscopy and one near-resonant HRS measurement. A key to reducing the number of measurements required is the use of symmetries and sum rules. This approach bridges the gulf between the two-level model, which misses important states, and multilevel models, that use adjustable parameters to fit the data or results of semi-empirical calculations that can not be directly validated by experiment.[41, 42] More importantly, our approach of combining theory with experiment leads to a small set of measured quantities that accurately predict the polarizability, hyperpolarizability, and second hyperpolarizability. Furthermore, our results show that we can model the nonlinear optical response in terms of “effective” broad bands that are composed of closely-lying or degenerate states and that are easily characterized from the linear absorption spectrum at room temperature.

Finally, we have proposed a new paradigm to increase the intrinsic nonlinear response of octupolar chromophores with  $D_{3h}$  symmetry, based on the inclusion of a central conjugated ring and the extension of the conjugated branches.

Our approach is generalizable to other systems using an analogous approach, provided that symmetries of the molecule exist that allow tensor components of the first (and second) hyperpolarizabilities to be related to each other. The sum rules, used in conjunction with dipole-free SOS expressions, can then be used to simplify the model so that a reduced number of quantities are required to fully characterize a molecule.

### Appendix A: Units in nonlinear optics

In this article we have used cgs-gaussian units to report the values of the second hyperpolarizability (Fig. 6) and other experimental values (Table I). This choice of units is motivated by the fact that in cgs-gaussian units, the polarization,  $\vec{P}$ , and the electric field strength,  $\vec{E}$ , have the same units ( $statV/cm$ ), and the second hyperpolariz-

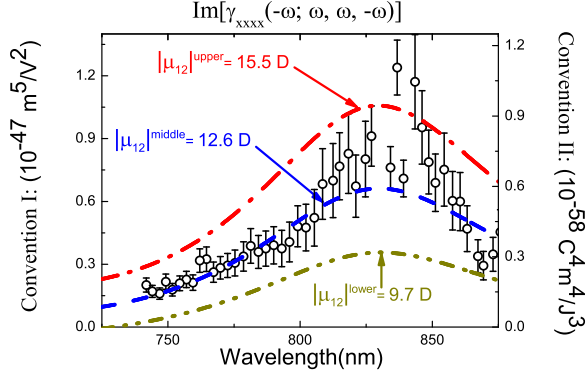


FIG. 7. (Color online) The measured spectrum of the imaginary part of the second hyperpolarizability (points) and the theoretical curve (middle), that is predicted from the measured value of  $\mu_{12}$  ( $|\mu_{12}|^{\text{middle}}$ ), in S.I. Convention I units (left axis) and in S.I. Convention II units (right axis). The upper and lower curves represent the uncertainty in the HRS-determined transition moment  $\mu_{12}$ . Note that there are *no adjustable parameters* in the theoretical modeling.

ability has units of ( $cm^5/statV^2$ ), sometimes referred to as *esu*. Traditionally, experimental values of the second hyperpolarizability have been reported in *esu* units.

In contrast, in S.I. units, the polarization has units of ( $C/m^2$ ) while the field strength has units of ( $V/m$ ), which has led to two possible different sets of units for the second hyperpolarizability, since in S.I. units there are two possible conventions for the definition of the nonlinear susceptibilities.[39] In the first convention (Convention I), the nonlinear susceptibilities are defined through:

$$P^{(n)} = \epsilon_0 \chi^{(n)}(E)^n, \quad (\text{A1})$$

where  $P^{(n)}$  is the  $n$ th-order polarization,  $\epsilon_0$  is the vacuum permittivity (in units of ( $F/m$ )),  $\chi^{(n)}$  is the  $n$ th-order nonlinear susceptibility and  $E$  is the electric field strength. In this convention, the units of the second hyperpolarizability are ( $m^5/V^2$ ).

In the second convention (Convention II), the nonlinear susceptibilities are defined through:

$$P^{(n)} = \chi^{(n)}(E)^n, \quad (\text{A2})$$

and the units of the second hyperpolarizability are ( $C^4 m^4 J^{-3}$ ).

For completeness, we plot the predicted dispersion and the experimental data points for the second hyperpolarizability in Fig. 7 using S.I. Convention I units (left axis); and using S.I. Convention II units (right axis).

Finally, in Table I, we have expressed the energies in units of electron Volts (eV) and the transition dipole moments in units of Debye (D). These are convenient units to describe molecular properties because all values are near unity in the same way that macroscopic values of

length and mass are near unity in SI units. A Debye is equal to  $10^{-18} statCm$  in cgs units, or approximately  $3.33564 \times 10^{-30} C.m$  in S.I. units, while an electron Volt is approximately  $1.602164 \times 10^{-12} erg$  in cgs units, and approximately  $1.602164 \times 10^{-19} J$  in S.I. units. In this appendix we report the energies and the transition dipole moments using strict cgs units (Table II) and using S.I. units (Table III).

## Appendix B: Finding the symmetry-adapted linear combinations (SALC) basis from the original basis set under for $D_{3h}$ symmetry and the allowed transition moments

In this appendix we use group theory to find the reducible representations that are spanned by the different choice of bases for the modeling of the AF-455 chromophore. The reducible representation is found by obtaining the character table for the different operations of the group for the chosen initial basis. From there, we can derive the symmetry-adapted linear combinations (SALC) basis. For details about the group theory calculations, please refer to the text by Cotton.[43].

### 1. Four initial bases

Consider an octupole that is modeled with four orthonormal bases  $|\phi_1\rangle$ ,  $|\phi_2\rangle$ ,  $|\phi_3\rangle$ , and  $|\phi_4\rangle$  as shown in Fig. 3 (top). Table IV shows the character table for the  $D_{3h}$  group. The reducible representation  $\Gamma_{red1}$  that results from this choice of basis set is presented in the last row of the character table.

Since we are only concerned with transition dipole moments that are allowed or disallowed, we will drop the last column of the character table for the rest of the appendix. Using group theory, the reducible representation can be reduced to two  $A_2''$  and one  $E''$  irreducible representations, and the Symmetry Adapted Linear Combinations (SALCs) can be obtained by applying projection operators of each of these irreducible representations on molecular orthonormal bases  $|\phi_1\rangle$  and  $|\phi_4\rangle$ . [43] The normalized SALCs are given by:

$$|g\rangle = \frac{1}{\sqrt{3}}(|\phi_1\rangle + |\phi_2\rangle + |\phi_3\rangle), \quad (\text{B1})$$

$$|e2\rangle = \frac{1}{\sqrt{6}}(2|\phi_1\rangle - |\phi_2\rangle - |\phi_3\rangle), \quad (\text{B2})$$

$$|e3\rangle = \frac{1}{\sqrt{2}}(|\phi_2\rangle - |\phi_3\rangle), \quad (\text{B3})$$

$$|e1\rangle = |\phi_4\rangle. \quad (\text{B4})$$

Group theory allows us to determine how many levels are degenerate, but does not tell us about the relative ordering of the levels in terms of their energy.  $|g\rangle$  and  $|e1\rangle$  are the ground state and the non-degenerate excited state, respectively, corresponding to two  $A_2''$  irreducible

$E_{10}$ (erg)	$E_{20}$ (erg)	$ \mu_{10} $ (statC.m)	$ \mu_{20} $ (statC.m)	$\Gamma_{10}$ (erg)	$\Gamma_{20}$ (erg)	$ \mu_{12} ^{\text{upper}}$ (statC.m)	$ \mu_{12} ^{\text{middle}}$ (statC.m)	$ \mu_{12} ^{\text{lower}}$ (statC.m)
$4.8 \times 10^{-12}$	$6.6 \times 10^{-12}$	$12.4 \times 10^{-18}$	$9.4 \times 10^{-18}$	$0.35 \times 10^{-12}$	$0.56 \times 10^{-12}$	$15.5 \times 10^{-18}$	$12.6 \times 10^{-18}$	$9.7 \times 10^{-18}$

TABLE II. Experimental parameters (from the linear absorption spectrum) and  $|\mu_{12}|$  measured using HRS in cgs units. The range of  $|\mu_{12}|$  values (upper, middle and lower) reflect the experimental uncertainties associated with HRS. All quantities are local-field corrected values.

$E_{10}$ (J)	$E_{20}$ (J)	$ \mu_{10} $ (C.m)	$ \mu_{20} $ (C.m)	$\Gamma_{10}$ (J)	$\Gamma_{20}$ (J)	$ \mu_{12} ^{\text{upper}}$ (C.m)	$ \mu_{12} ^{\text{middle}}$ (C.m)	$ \mu_{12} ^{\text{lower}}$ (C.m)
$4.8 \times 10^{-17}$	$6.6 \times 10^{-17}$	$4.2 \times 10^{-29}$	$3.14 \times 10^{-29}$	$0.35 \times 10^{-17}$	$0.56 \times 10^{-17}$	$5.17 \times 10^{-29}$	$4.2 \times 10^{-29}$	$3.24 \times 10^{-29}$

TABLE III. Experimental parameters (from the linear absorption spectrum) and  $|\mu_{12}|$  measured using HRS in S.I. units. The range of  $|\mu_{12}|$  values (upper, middle and lower) reflect the experimental uncertainties associated with HRS. All quantities are local-field corrected values.

representations, and  $|e2\rangle$  and  $|e3\rangle$  are two degenerate excited states corresponding to the  $E''$  irreducible representation. The position of the state  $|e1\rangle$  is chosen arbitrarily in Fig. 3 (bottom), which has no significance in our calculations.

We summarize the possible transition moments, direct products of the corresponding irreducible representations, and the calculated characters in Table V.

A transition moment is allowed only if the direct product is or contains the totally symmetric irreducible representation, for instance,  $A_1'$  in  $D_{3h}$  symmetry. Therefore the x-, y-allowed transition moments are given in Table VI, as shown also in Fig 3 (bottom).

## 2. Six-state initial basis

Now we consider six orthonormal bases  $|\phi_1\rangle, |\phi_2\rangle, |\phi_3\rangle, |\phi_4\rangle, |\phi_5\rangle$ , and  $|\phi_6\rangle$  as shown in Fig. 4. Following the same procedure as in the case of 4 initial basis (section B 1, we obtain the following SALCs:

$$|g\rangle = \frac{1}{\sqrt{3}}(|\phi_5\rangle + |\phi_6\rangle + |\phi_4\rangle), \quad (\text{B5})$$

$$|e1\rangle = \frac{1}{\sqrt{3}}(|\phi_1\rangle + |\phi_2\rangle + |\phi_3\rangle), \quad (\text{B6})$$

$$|e2\rangle = \frac{1}{\sqrt{6}}(2|\phi_1\rangle - |\phi_2\rangle - |\phi_3\rangle), \quad (\text{B7})$$

$$|e3\rangle = \frac{1}{\sqrt{2}}(|\phi_2\rangle - |\phi_3\rangle), \quad (\text{B8})$$

$$|e4\rangle = \frac{1}{\sqrt{6}}(2|\phi_5\rangle - |\phi_6\rangle - |\phi_4\rangle), \quad (\text{B9})$$

$$|e5\rangle = \frac{1}{\sqrt{2}}(|\phi_6\rangle - |\phi_4\rangle). \quad (\text{B10})$$

Table VII shows the character table for the  $D_{3h}$  group. The reducible representation  $\Gamma_{red2}$  that results from this choice of basis set is presented in the last row of the character table.

Table VIII shows the possible transition moments, direct products of the corresponding irreducible representations, and the calculated characters.

Finally, we can calculate the allowed x-, y- transition moments. The x-, y-allowed transition moments are between  $|g\rangle$  and  $|e2, e3\rangle$ ,  $|g\rangle$  and  $|e4, e5\rangle$ ,  $|e1\rangle$  and  $|e2, e3\rangle$ ,  $|e1\rangle$  and  $|e4, e5\rangle$ ,  $|e2\rangle$  and  $|e3\rangle$ ,  $|e2, e3\rangle$  and  $|e4, e5\rangle$ , and  $|e4\rangle$  and  $|e5\rangle$ , as shown in Fig. 4. x- or y- transitions between  $|g\rangle$  and  $|e1\rangle$  are forbidden.

## ACKNOWLEDGMENTS

JPM acknowledges the Fund for Scientific Research Flanders (FWO) and the K.U.Leuven IDO project 3E090505. MGK thanks the National Science Foundation (ECS-0756936) and Wright Patterson Air Force Base for generously supporting this work. We thank Wright Patterson AFB for supplying the AF-455 chromophore used in these studies. KC acknowledges FWO grant G.0312.08

[1] R. W. Hellwarth, A. Owyong, and N. George, "Origin of the Nonlinear Refractive Index of Liquid  $CCl_4$ ," Phys.

Rev. A **4**, 2342–2347 (1971).

[2] B. I. Greene and R. C. Farrow, "Direct Measurement of a

- Subpicosecond Birefringent Response in  $CS_2$ ,” J. Chem. Phys. **77**, 4779–4783 (1982).
- [3] B. I. Greene, P. A. Fleury, J. H. L. Carter, and R. C. Farrow, “Microscopic Dynamics in Simple Liquids by Subpicosecond Birefringences,” Phys. Rev. A **29**, 271–4 (1984).
- [4] J. Etchepare, G. Grillon, G. Hamoniaux, A. Antonetti, and A. Orszag, “Molecular Dynamics of Liquid Benzene via Femtosecond Pulse Laser Excitation,” Rev. Phys. Appl. **22**, 1749–53 (1987).
- [5] J. Etchepare, G. Grillon, A. Migus, J. L. Martin, and G. Hamoniaux, “Efficient Femtosecond Optical Kerr Shutter,” Appl. Phys. Lett. **43**, 406–407 (1983).
- [6] B. I. Greene, J. Orenstein, R. R. Millard, and L. R. Williams, “Nonlinear Optical Response of Excitons Confined to One Dimension,” Phys. Rev. Lett. **58**, 2750–53 (1987).
- [7] B. I. Greene, J. F. Mueller, J. Orenstein, D. H. Rapkine, S. Schmitt-Rink, and M. Thakur, “Phonon-Mediated Optical Nonlinearity in Polydiacetylene,” Phys. Rev. Lett. **61**, 325–28 (1988).
- [8] M. G. Kuzyk, R. A. Norwood, J. W. Wu, and A. F. Garito, “Frequency dependence of the optical Kerr effect and third-order electronic nonlinear-optical processes of organic liquids,” J. Opt. Soc. Am. B **6**, 154–64 (1989).
- [9] B. J. Orr and J. F. Ward, “Perturbation Theory of the Non-Linear Optical Polarization of an Isolated System,” Mol. Phys. **20**, 513–526 (1971).
- [10] S. R. Vigil and M. G. Kuzyk, “Absolute molecular optical Kerr effect spectroscopy of dilute organic solutions and neat organic liquids,” J. Opt. Soc. Am. B **18**, 679–691 (2001).
- [11] A. M. Kelley, “Frequency-dependent first hyperpolarizabilities from linear absorption spectra,” J. Opt. Soc. Am. B **19**, 1890–1900 (2002).
- [12] S. Bidault, S. Brasselet, J. Zyss, O. Maury, and H. Le Bozec, “Role of spatial distortions on the quadratic nonlinear optical properties of octupolar organic and metallo-organic molecules,” J. Chem. Phys. **126**, 034312 (2007).
- [13] S. Brasselet and J. Zyss, “Relation between quantum and geometric dimensionalities in molecular nonlinear optics: Beyond the two-level model for anisotropic systems,” Journal of Nonlinear Optical Physics and Materials **5**, 671–694 (1996).
- [14] J. Weibel, D. Yaron, and J. Zyss, “Quantum and tensorial modeling of multipolar nonlinear optical chromophores by a generalized equivalent internal potential,” J. Chem. Phys. **119**, 11847 (2003).
- [15] J. Pérez Moreno, *Theoretical and experimental characterization of the first hyperpolarizability*, Ph.D. thesis, Washington State University & K.U.Leuven (2007).
- [16] J. Pérez-Moreno and K. Clays, “Fundamental Limits: Developing New Tools for a Better Understanding of Second-Order Molecular Nonlinear Optics,” Journal of Nonlinear Optical Physics and Materials **18**, 401–440 (2009).
- [17] M. G. Kuzyk, “Physical Limits on Electronic Nonlinear Molecular Susceptibilities,” Phys. Rev. Lett. **85**, 1218–1221 (2000).
- [18] M. G. Kuzyk, “Quantum limits of the hyper-Rayleigh scattering susceptibility,” IEEE Journal on Selected Topics in Quantum Electronics **7**, 774–780 (2001).
- [19] M. G. Kuzyk, “Erratum: Physical Limits on Electronic Nonlinear Molecular Susceptibilities,” Phys. Rev. Lett. **90**, 039902 (2003).
- [20] M. G. Kuzyk, “Compact sum-over-states expression without dipolar terms for calculating nonlinear susceptibilities,” Phys. Rev. A **72**, 053819 (2005).
- [21] J. Pérez-Moreno, K. Clays, and M. G. Kuzyk, “A new dipole-free sum-over-states expression for the second hyperpolarizability,” J. Chem. Phys. **128**, 084109 (2008).
- [22] J. Pérez Moreno and M. G. Kuzyk, “Fundamental limits of the dispersion of the two-photon absorption cross section,” J. Chem. Phys. **123**, 194101 (2005).
- [23] A. Rebane, N. S. Makarov, M. Drobizhev, B. Spangler, E. S. Tarter, B. D. Reeves, C. W. Spangler, F. Meng, and Z. Suo, “Quantitative Prediction of Two-Photon Absorption Cross Section Based on Linear Spectroscopic Properties,” J. Phys. Chem. C **112**, 7997–8004 (2008).
- [24] W. Thomas, “Über die Zahl der Dispersionselektronen, die einem stationären Zustande zugeordnet sind. (Vorläufige Mitteilung),” Naturwissenschaften **13**, 627–627 (1925).
- [25] W. Kuhn, “Über die Gesamtstärke der von einem Zustande ausgehenden Absorptionslinien,” Zeitschrift für Physik A Hadrons and Nuclei **33**, 408–412 (1925).
- [26] W. Heisenberg, “Über quantentheoretische Umdeutung kinematischer und mechanischer Beziehungen,” Zeitschrift für Physik A Hadrons and Nuclei **33**, 879–893 (1925).
- [27] M. Cho, H. Kim, and S. Jeon, “An elementary description of nonlinear optical properties of octupolar molecules: Four-state model for guanidinium-type molecules,” J. Chem. Phys. **108**, 7114 (1998).
- [28] W. Lee, H. Lee, J. Kim, J. Choi, M. Cho, S. Jeon, and B. Cho, “Two-photon absorption and nonlinear optical properties of octupolar molecules,” J. Am. Chem. Soc. **123**, 10658–10667 (2001).
- [29] M. Joffre, D. Yaron, J. Silbey, and J. Zyss, “Second Order Optical Nonlinearity in Octupolar Aromatic Systems,” J. Chem. Phys. **97**, 5607–5615 (1992).
- [30] K. Tripathy, J. Pérez Moreno, M. G. Kuzyk, B. J. Coe, K. Clays, and A. M. Kelley, “Why hyperpolarizabilities Fall Short of the Fundamental Quantum Limits,” J. Chem. Phys. **121**, 7932–7945 (2004).
- [31] K. Clays and A. Persoons, “Hyper-Rayleigh Scattering in Solution,” Phys. Rev. Lett. **66**, 2980–2983 (1991).
- [32] K. Clays and A. Persoons, “Hyper-Rayleigh Scattering in Solution,” Rev. Sci. Instrum. **63**, 3285–3289 (1992).
- [33] S. Kielich and R. Zawodny, “Tensor Relationship of the Molecular Electric Multipole Moments for all Point Group Symmetries,” Chem. Phys. Lett. **12**, 20–23 (1971).
- [34] G. Olbrechts, R. Strobbe, K. Clays, and A. Persoons, “High-frequency demodulation of multi-photon fluorescence in hyper-Rayleigh scattering,” Rev. Sci. Instrum. **69**, 2233 (1998).
- [35] C. Xu and W. W. Webb, “Measurement of two-photon excitation cross sections of molecular fluorophores with data from 690 to 1050 nm,” J. Opt. Soc. Am. **13**, 481–491 (1996).
- [36] D. A. Oulianov, I. V. Tomov, A. S. Dvornikov, and P. M. Rentzepis, “Observations onto the measurement of two-photon absorption cross-sections,” Opt. Commun. **191**, 235–243 (2001).
- [37] R. L. Sutherland, M. C. Brant, J. Heinrichs, J. E. Rogers, J. E. Slagle, D. G. McKean, and P. A. Fleitz, “Excited-state characterization and effective three-photon absorption model of two-photon-induced excited-state absorp-

- tion in organic pushpull charge-transfer chromophores,” *J. Opt. Soc. Am. B* **22**, 1939–1948 (2005).
- [38] K. D. Belfield, M. Bondar, F. E. Hernandezt, O. V. Przhonska, and S. Yao, “Two-photon absorption cross section determination for fluorene derivatives: Analysis of the methodology and elucidation of the origin of the absorption processes,” *J. Phys. Chem. B* **111**, 12723–12729 (2007).
- [39] M. G. Kuzyk and C. W. Dirk, *Characterization techniques and tabulations for organic nonlinear optical materials* (Marcel Dekker, 1998).
- [40] M. C. Kuzyk and M. G. Kuzyk, “Monte Carlo Studies of the Fundamental Limits of the Intrinsic Hyperpolarizability,” *J. Opt. Soc. Am. B* **25**, 103–110 (2008).
- [41] J. Fu, A. P. Lazaro, D. J. Hagan, E. W. Van Stryland, O. V. Przhonska, M. V. Bondar, Y. L. Slominsky, and A. D. Kachkovski, “Molecular structure – two-photon absorption property relations in polymethine dyes,” *J. Opt. Soc. Am. B* **24**, 56–66 (2007).
- [42] J. Fu, A. P. Lazaro, D. J. Hagan, E. W. Van Stryland, O. V. Przhonska, M. V. Bondar, Y. L. Slominsky, and A. D. Kachkovski, “Experimental and theoretical approaches to understanding two-photon absorption spectra in polymethine and squaraine molecules,” *J. Opt. Soc. Am. B* **24**, 67–76 (2007).
- [43] F. A. Cotton, *Chemical Applications of Group Theory, 3rd Edition* (John Wiley & Sons, Inc., 1990).

TABLE IV. The character table for the  $D_{3h}$  group. The reducible representation  $\Gamma_{red1}$  that results from the choice of 4 basis shown in Fig. 3 is presented in the last row.

$D_{3h}$	$E$	$2C_3$	$3C_2$	$\sigma_h$	$2S_3$	$3\sigma_v$		
$A_1'$	1	1	1	1	1	1		$x^2 + y^2, z^2$
$A_2'$	1	1	-1	1	1	-1	$R_z$	
$E'$	2	-1	0	2	-1	0	$(x, y)$	$x^2 - y^2, xy$
$A_1''$	1	1	1	-1	-1	-1		
$A_2''$	1	1	-1	-1	-1	1	$z$	
$E''$	2	-1	0	-2	1	0	$(R_x, R_y)$	$xz, yz$
$\Gamma_{red1}$	4	1	-2	-4	-1	2		

TABLE V. Possible transition moments, direct products of the corresponding irreducible representations, and the calculated characters for different operations of the group, that result from the choice of 4 basis presented in Fig. 3.

	$D_{3h}$	$E$	$2C_3$	$3C_2$	$\sigma_h$	$2S_3$	$3\sigma_v$		
	$A_1'$	1	1	1	1	1	1		$x^2 + y^2, z^2$
	$A_2'$	1	1	-1	1	1	-1	$R_z$	
	$E'$	2	-1	0	2	-1	0	$(x, y)$	$x^2 - y^2, xy$
	$A_1''$	1	1	1	-1	-1	-1		
	$A_2''$	1	1	-1	-1	-1	1	$z$	
	$E''$	2	-1	0	-2	1	0	$(R_x, R_y)$	$xz, yz$
$\langle g (x, y) e1\rangle$	$A_2'' E' A_2''$	2	-1	0	2	-1	0		
$\langle g (x, y) e2, e3\rangle$	$A_2'' E' E''$	4	1	0	4	1	0		
$\langle e1 (x, y) e2, e3\rangle$	$A_2'' E' E''$	4	1	0	4	1	0		
$\langle e2, e3 (x, y) e2, e3\rangle$	$E'' E' E''$	8	-1	0	8	-1	0		
$\langle g z e1\rangle$	$A_2'' A_2'' A_2''$	1	1	-1	-1	-1	1		
$\langle g z e2, e3\rangle$	$A_2'' A_2'' E''$	2	-1	0	-2	1	0		
$\langle e1 z e2, e3\rangle$	$A_2'' A_2'' E''$	2	-1	0	-2	1	0		
$\langle e2, e3 z e2, e3\rangle$	$E'' A_2'' E''$	4	1	0	-4	-1	0		

TABLE VI. Allowed transition moments for the irreducible representation spanned by the initial choice of 4 basis presented in Fig. 3.

$\langle g (x, y) e2, e3\rangle$	$\langle e1 (x, y) e2, e3\rangle$	$\langle e2 (x, y) e3\rangle$
$\langle e2, e3 (x, y) g\rangle$	$\langle e2, e3 (x, y) e1\rangle$	$\langle e3 (x, y) e2\rangle$

TABLE VII. The character table for the  $D_{3h}$  group and the reducible representation  $\Gamma_{red2}$  that results from the choice of 6 basis shown in Fig. 4.

$D_{3h}$	$E$	$2C_3$	$3C_2$	$\sigma_h$	$2S_3$	$3\sigma_v$		
$A_1'$	1	1	1	1	1	1		$x^2 + y^2, z^2$
$A_2'$	1	1	-1	1	1	-1	$R_z$	
$E'$	2	-1	0	2	-1	0	$(x, y)$	$x^2 - y^2, xy$
$A_1''$	1	1	1	-1	-1	-1		
$A_2''$	1	1	-1	-1	-1	1	$z$	
$E''$	2	-1	0	-2	1	0	$(R_x, R_y)$	$xz, yz$
$\Gamma_{red2}$	6	0	-2	-6	0	2		

TABLE VIII. Possible transition moments, direct products of the corresponding irreducible representations, and the calculated characters the for different operations of the group, that result from the choice of 6 basis presented in Fig. 4.

	$D_{3h}$	$E$	$2C_3$	$3C_2$	$\sigma_h$	$2S_3$	$3\sigma_v$		
	$A_1'$	1	1	1	1	1	1		$x^2 + y^2, z^2$
	$A_2'$	1	1	-1	1	1	-1	$R_z$	
	$E'$	2	-1	0	2	-1	0	$(x, y)$	$x^2 - y^2, xy$
	$A_1''$	1	1	1	-1	-1	-1		
	$A_2''$	1	1	-1	-1	-1	1	$z$	
	$E''$	2	-1	0	-2	1	0	$(R_x, R_y)$	$xz, yz$
$\langle g (x, y) e1\rangle$	$A_2'' E' A_2''$	2	-1	0	2	-1	0		
$\langle g (x, y) e2, e3\rangle$	$A_2'' E' E''$	4	1	0	4	1	0		
$\langle g (x, y) e4, e5\rangle$	$A_2'' E' E''$	4	1	0	4	1	0		
$\langle e1 (x, y) e2, e3\rangle$	$A_2'' E' E''$	4	1	0	4	1	0		
$\langle e1 (x, y) e4, e5\rangle$	$A_2'' E' E''$	4	1	0	4	1	0		
$\langle e2, e3 (x, y) e2, e3\rangle$	$E'' E' E''$	8	-1	0	8	-1	0		
$\langle e2, e3 (x, y) e4, e5\rangle$	$E'' E' E''$	8	-1	0	8	-1	0		
$\langle e4, e5 (x, y) e4, e5\rangle$	$E'' E' E''$	8	-1	0	8	-1	0		
$\langle g z e1\rangle$	$A_2'' A_2'' A_2''$	1	1	-1	-1	-1	1		
$\langle g z e2, e3\rangle$	$A_2'' A_2'' E''$	2	-1	0	-2	1	0		
$\langle g z e4, e5\rangle$	$A_2'' A_2'' E''$	2	-1	0	-2	1	0		
$\langle e1 z e2, e3\rangle$	$A_2'' A_2'' E''$	2	-1	0	-2	1	0		
$\langle e1 z e4, e5\rangle$	$A_2'' A_2'' E''$	2	-1	0	-2	1	0		
$\langle e2, e3 z e2, e3\rangle$	$E'' A_2'' E''$	4	1	0	-4	-1	0		
$\langle e2, e3 z e4, e5\rangle$	$E'' A_2'' E''$	4	1	0	-4	-1	0		
$\langle e4, e5 z e4, e5\rangle$	$E'' A_2'' E''$	4	1	0	-4	-1	0		